

Integrative MultiOmics and Machine Learning Reveal Peroxiredoxin 4 as a Critical Hub Governing Mitochondrial Dysfunction and B Cell Differentiation in Periodontitis

Congyi Tu^{1,*}, Yaxian Luo^{2,*}, Tianle Jiang^{1,*}, Zhan Yang^{1,3,*}, Bingqian Yang², Kechen Zhang¹, Jingyu Zhang², Chaoming Hu¹, Lijun Zhou³, Tao Qiu², Haorong Xia¹, Ziyu Xi¹, Rongdang Hu¹, Mouyuan Sun²

¹Institute of Stomatology, School and Hospital of Stomatology, Wenzhou Medical University, Wenzhou, Zhejiang, People's Republic of China; ²Stomatology Hospital, School of Stomatology, Zhejiang University School of Medicine, Zhejiang Provincial Clinical Research Center for Oral Diseases, Zhejiang Key Laboratory of Oral Biomedical, Hangzhou, Zhejiang, People's Republic of China; ³Department of Dentistry, Yongkang First People's Hospital of Wenzhou Medical University, Jinhua, Zhejiang, People's Republic of China

*These authors contributed equally to this work

Correspondence: Mouyuan Sun; Rongdang Hu, Email sunmouyuan777@zju.edu.cn; hurongdang@wmu.edu.cn

Aim: Periodontitis, a highly prevalent chronic inflammatory disease, progressively destroys tooth-supporting tissues, ultimately leading to tooth loss, and significantly increases systemic risks such as cardiovascular disease and diabetic complications. Current mechanical therapies effectively control clinical symptoms but fail to eradicate pathogenic microenvironments or restore periodontal homeostasis. Mitochondrial dysfunction is a critical driver of periodontitis progression; however, the regulatory mechanisms of mitochondria-related genes remain poorly defined.

Materials and Methods: This study integrated bulk transcriptome sequencing (bulk RNA-seq) and single-cell RNA-seq (scRNA-seq) analyses to identify mitochondrial dysfunction-associated immune cell alterations in periodontitis. Key mitochondria-related genes inducing disease progression were pinpointed through non-negative matrix factorization (NMF) and weighted gene coexpression network analysis (WGCNA). By integrating ten machine learning algorithms with experimental validation using real-time quantitative polymerase chain reaction (qPCR) and immunofluorescence, peroxiredoxin 4 (PRDX4) was identified as the most crucial hub gene governing mitochondrial homeostasis in periodontitis.

Results: Patient stratification based on PRDX4 expression revealed upregulated B cell-related pathways. Pseudotime analysis demonstrated a synchronized upregulation of PRDX4 and B cell signature genes during late-stage disease progression. scRNA-seq and immunofluorescence confirmed PRDX4 upregulation in B cells, particularly in plasma cells and memory B cells, and indicated its involvement in B cell differentiation. Experiments in a mouse model further validated the conserved functional role of PRDX4 in regulating B cells during periodontitis. Finally, we screened traditional Chinese medicinal compounds and identified aloe as a potential PRDX4 inhibitor.

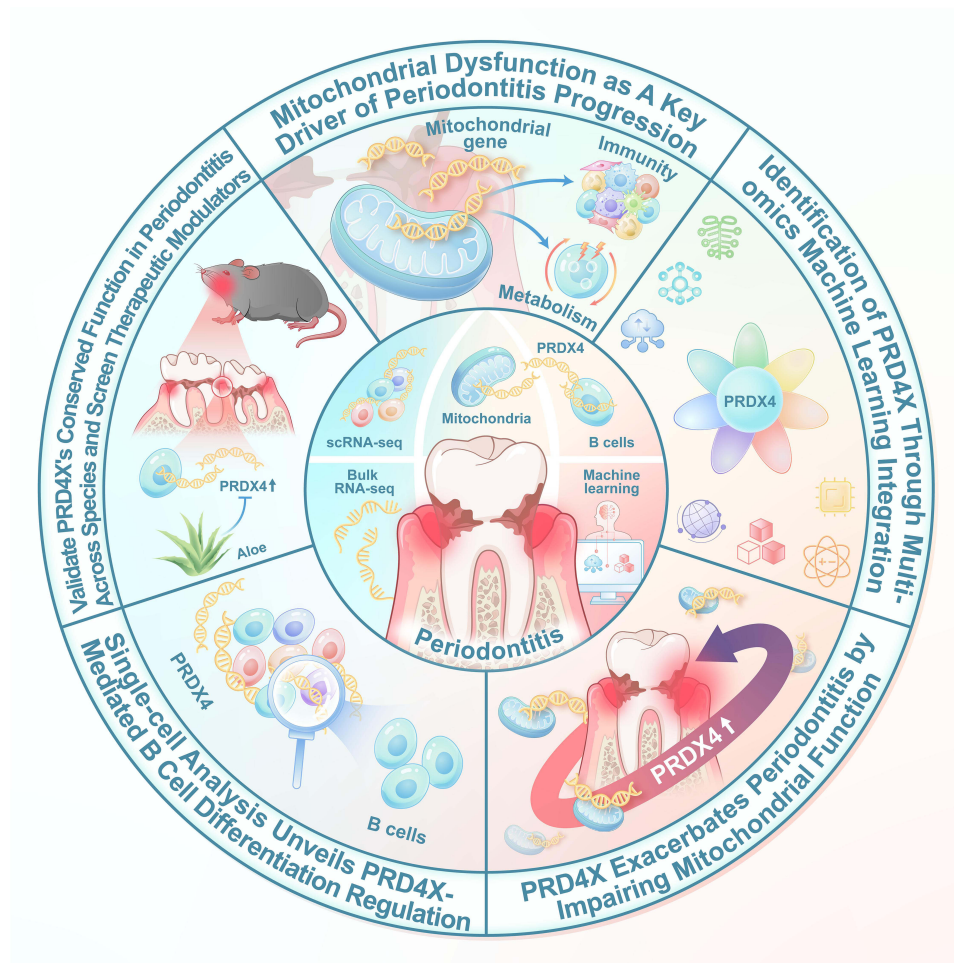
Conclusion: These findings establish PRDX4 as a key regulatory node linking mitochondrial dysfunction to periodontitis pathogenesis, providing insights into mitochondria-related genes and potential therapeutic strategies.

Keywords: periodontitis, mitochondria, B cell, multi-omics, PRDX4

Introduction

Periodontitis, a chronic inflammatory disease initiated by periodontal bacteria, is characterized by the progressive destruction of tooth-supporting tissues, ultimately leading to tooth loss.^{1,2} It severely impairs the oral function, aesthetics, and quality of life, while increasing systemic risks such as cardiovascular disease and diabetic complications.^{3,4} The

Graphical Abstract



World Health Organization's Global Oral Health Status Report (2022) highlights its pandemic scale, estimating that nearly 3.5 billion people suffer from oral diseases, with periodontitis being the most prevalent.⁵ These figures underscore an urgent need for global prevention and early intervention strategies to mitigate its individual and societal burden. Current therapeutic strategies for periodontitis, including mechanical debridement, antimicrobial agents, and regenerative surgery, primarily aim to disrupt pathogenic biofilms and suppress local inflammation.^{6–9} However, these approaches demonstrate inherent limitations: they achieve only transient control of clinical symptoms and fail to fundamentally disrupt pathogenic host–microbe interactions, eradicate the persistent inflammatory microenvironment, or enable functional tissue regeneration.^{9–11} Consequently, while these interventions might slow disease progression, they cannot restore disrupted periodontal homeostasis or prevent recurrence. This underscores the urgent need to elucidate the molecular mechanisms underlying microenvironmental dysregulation and tissue destruction, thereby identifying novel therapeutic targets to complement conventional mechanotherapies with precise, biology-driven interventions.

Mitochondrial dysfunction serves as a pivotal driver of periodontitis pathogenesis, bridging microbial aggression, immune dysregulation, and tissue degeneration.^{12,13} Mitochondrial dysfunction—manifested by the mitochondrial calcium (mito Ca^{2+}) overload, accumulation of mitochondrial reactive oxygen species (mROS), adenosine triphosphate (ATP) depletion, activation of the mitochondrial permeability transition (mPT), and impaired mitophagy—directly contributes to inflammatory tissue damage and impaired tissue regeneration.^{14,15} Mitochondrial calcium signaling and redox imbalance have been mechanistically linked to dysregulated osteoclast, osteoblast differentiation, and connective

tissue cell apoptosis.^{16,17} mPT triggers the release of mitochondrial DNA (mtDNA), N-formyl peptides, and mROS, which exacerbate immune cell activation and perpetuate inflammation.¹⁸ Although evidence underscores mitochondria as a central node in periodontitis pathogenesis, the precise mechanisms by which the myriad mitochondrial genes orchestrate the dysregulated microenvironment remain poorly defined. Given the strong correlation between mitochondrial structural damage in periodontal tissues and disease severity,^{13,19} targeting mitochondria-associated molecular pathways might represent a precise strategy to disrupt the vicious cycle of microenvironmental dysregulation. Deciphering mitochondria-related gene networks thus emerges as an urgent priority to unravel the complexity of mitochondrial contributions to periodontitis and identify novel therapeutic targets for restoring periodontal homeostasis.

With the rapid advancement of multiomics technologies, bulk RNA-seq enables the systematic capture of gene expression signatures in periodontal tissues, particularly facilitating the identification of disease-specific upregulated genes and their correlations with mitochondria-related genes.^{20,21} In parallel, scRNA-seq provides unprecedented resolution to directly delineate the cell-type-specific expression patterns of key mitochondrial genes and their regulatory networks across distinct cellular subpopulations, revolutionizing our understanding of cellular heterogeneity within complex tissues such as periodontal tissues.²² Thus, the functional enrichment analysis of scRNA-seq data identifies key biological pathways and processes dysregulated in disease states and further delineates dysregulated mitochondrial pathways.²³ Pseudotime analysis additionally reconstructs dynamic cellular trajectories, revealing the transitional states and molecular drivers of disease progression.²⁴ To harness the high dimensionality and complexity of these multiomics datasets, multiple machine learning approaches are increasingly used.^{25,26} Supported by these machine learning methodologies, the development of precision medicine has achieved unprecedented growth. These technologies also facilitate the discovery of novel biomarker signatures that help elucidate the molecular underpinnings of disease. This synergistic integration of bulk RNA-seq, scRNA-seq, trajectory inference, and advanced machine learning analytics provides a powerful, multifaceted framework for dissecting the molecular pathophysiology of periodontitis.

Given the critical yet poorly defined role of mitochondrial dysfunction in the pathogenesis of periodontitis, we leveraged an integrative framework combining multi-omics technologies and machine learning to systematically decipher mitochondria-related molecular mechanisms. However, a comprehensive understanding of how mitochondrial gene networks regulate the immune microenvironment and drive disease progression is still lacking. To address this need, this study was designed to systematically identify and validate key mitochondrial regulators in periodontitis. We applied weighted gene coexpression network analysis and non-negative matrix factorization clustering to identify disease subtypes and key genes, employed multiple machine learning algorithms to pinpoint peroxiredoxin 4 (PRDX4) as a central hub gene governing mitochondrial homeostasis, and subsequently validated its critical role in B-cell function through single-cell analysis and animal models. Furthermore, we explored the therapeutic potential of PRDX4 by screening natural compounds targeting this pathway. Collectively, these findings establish PRDX4 as a key regulatory node linking mitochondrial dysfunction to periodontitis pathogenesis and provide a foundation for novel therapeutic strategies.

Materials and Methods

Bulk RNA-Seq Data Processing and Analysis

Differential expression analysis between periodontitis patients and healthy controls was performed using the limma R package.²⁷ Genes with an adjusted p-value <0.05 (Benjamini–Hochberg method) were considered differentially expressed. For pathway analysis, Gene ontology (GO) and Kyoto encyclopedia of genes and genomes (KEGG) enrichment analyses were conducted using the clusterProfiler software package.²⁸ Three GO categories were examined: biological process (BP), cellular components (CC), and molecular function (MF). Additionally, metabolism-related pathway analysis was performed using gene set variation analysis (GSVA) and single-sample gene set enrichment analysis (ssGSEA) with R package GSVA²⁹ and ssGSEA,³⁰ with metabolism-related gene sets obtained from the R package scMetabolism.³¹

A comprehensive correlation analysis was performed using the Spearman rank correlation to explore relationships among mitochondrial, immune, and metabolism-related genes. WGCNA was conducted on the differentially expressed genes to identify gene modules associated with periodontitis, using the WGCNA R package.³² Module eigengenes were

calculated and correlated with clinical traits via Pearson correlation. The WGCNA analysis used several R packages: matrixStats, Hmisc, foreach, doParallel, fastcluster, DynamicTreeCut, survival, and WGCNA.

Network Analysis and Disease Subtyping

Potential molecular isoforms were identified through the non-negative matrix factorization (NMF) clustering of differentially expressed genes using the survival and NMF R packages.³³ The optimal number of clusters was determined by evaluating the cophenetic correlation coefficient, dispersion, and silhouette width metrics. The clustering results were visualized using t-distributed stochastic neighbor embedding. Sample pseudotime indexing was performed by applying principal component analysis (PCA) with a three-knot B-spline fit to the first two components, assigning each sample a developmental time units value scaled from 0.0 to 10.0.

Immune Microenvironment Analysis

The immune landscape was characterized using multiple computational approaches. CIBERSORT, with the LM22 signature matrix, was used to estimate the relative abundance of 22 immune cell subtypes within the mixed cell populations.³⁴ To validate these results, xCell was applied for cell type enrichment analysis, and ssGSEA was performed to quantify immune-related pathway activities.³⁵ The analysis incorporated 29 immune-related gene signatures, and results were compared between periodontitis and healthy control groups using linear models with empirical Bayes moderation.

Machine Learning Analysis

The integrated dataset was analyzed using a comprehensive set of ten distinct machine learning algorithms to ensure robust feature selection.³⁶ The models employed were Logistic Regression (LR), Support Vector Machine (SVM), Neural Network (NNET), Gradient Boosting Machine (GBM), Random Forest (RF), Extreme Gradient Boosting (XGB), K-Nearest Neighbors (KNN), Adaptive Boosting (ADA), Classification and Regression Trees (CART), and Multilayer Perceptron (MLP). To identify the most predictive features, we performed feature selection using Least Absolute Shrinkage and Selection Operator (LASSO) regression (Table 1). The performance of each model was rigorously evaluated via 10-fold cross-validation. The assessment was based on multiple metrics derived from Receiver Operating Characteristic (ROC) curve analysis, confusion matrices, calibration curves, and Decision Curve Analysis (DCA). The optimal model was subsequently selected based on its comprehensive performance for further biological validation.

RT-qPCR Analysis

Total RNA was extracted using the TRIzol reagent (Invitrogen, USA) to validate the reliability of key prognostic genes in periodontal tissues. Human samples were obtained from periodontitis-affected gingival tissues and adjacent healthy gingival tissues collected during tooth extraction. Mouse samples were collected from periodontitis-induced lesions and contralateral

Table 1 R Packages Employed for Each Machine Learning Algorithm

Algorithm	R Package
Logistic Regression (LR)	Stats, glmnet
Support Vector Machine (SVM)	e1071, kernlab
Neural Network (NNET)	nnet
Gradient Boosting Machine (GBM)	gbm
Random Forest (RF)	RandomForest
Extreme Gradient Boosting (XGB)	xgboost
K-Nearest Neighbors (KNN)	Class, kkn
Adaptive Boosting (ADA)	adabag
Classification and Regression Trees (CART)	rpart
Multilayer Perceptron (MLP)	nnet

healthy periodontal tissues. RT-qPCR analysis was performed using the primers listed in Table 2, with glyceraldehyde-3-phosphate dehydrogenase (GAPDH) as the endogenous control for human samples and β -actin for mouse samples.

Immunofluorescence

Paraffin sections were blocked with bovine serum albumin and then incubated overnight in a humidified chamber at 4°C with primary antibodies (anti-PRDX4 and anti-CD20). The slides were subsequently incubated with a fluorescein-conjugated secondary antibody for 1 h under dark conditions at room temperature. Cell nuclei were counterstained with 4',6-diamidino-2-phenylindole (DAPI). Imaging was performed using a ZEISS confocal microscope. The antibodies used were anti-PRDX4 (Proteintech, Wuhan, China; 60286-1-Ig) and anti-CD20 (Abcam, Cambridge, UK; ab64088).

Animal Experimental Periodontitis Models

All animal experiments were approved by the Animal Ethics Committee of Zhejiang Center of Laboratory Animals (ZJCLA-IACUC-20011430) and were conducted in accordance with the Guide for the Care and Use of Laboratory Animals (National Research Council, 1996). Seven-week-old male C57BL/6 mice were randomly assigned to two groups: Group C (untreated control) and Group P (experimental periodontitis induction). Periodontitis was induced by ligating a 5–0 silk suture around the cervical region of the maxillary second molar for 7 d. Briefly, mice were anesthetized and immobilized, and the suture was positioned at the cervical margin of the target molar using ophthalmic forceps. Sutures were inspected every 2 d, and if loosening was detected, religation was performed immediately.

Collection of Human Periodontal Tissues

All human gingival tissue samples were collected under a protocol approved by the relevant Ethics Committee (Approval No: EC2025-LW-016-01(K)), with written informed consent obtained from all participants. Strict exclusion criteria were applied, including smoking, diabetes, cardiovascular diseases, chronic inflammatory or autoimmune conditions, recent antibiotic use, long-term medication history, and other systemic factors that could confound periodontal inflammation. Participants were divided into two groups: Healthy controls, whose tissues were obtained from sites with probing depth (PD) \leq 3 mm, no bleeding on probing (BOP), no clinical attachment loss (CAL), and no radiographic evidence of bone loss; and Periodontitis patients, whose tissues were collected from diseased sites with PD \geq 5 mm, CAL \geq 3 mm, and significant radiographic bone resorption exceeding the coronal third (during flap surgery or extraction of periodontally compromised teeth). Gingival biopsies (approximately 5×2.5 mm) were immediately placed in sterile saline-containing specimen bags, labeled with patient identifiers, and stored with recorded clinical parameters.

Statistical Methods

All statistical analyses were performed using R (version 4.2.1) and GraphPad Prism (version 9.0). Continuous variables were compared between two groups using Student's *t*-test for normally distributed data or the Mann–Whitney *U*-test for non-normally distributed data. The Spearman correlation coefficient was used to assess rank correlations between variables. Bivariate associations for nonparametric data were also evaluated using Spearman rank correlation. Survival

Table 2 All the Primers Used in the RT-qPCR Analysis

	Forward: 5' to 3'	Reverse Primer: 3' to 5'
PRDX4	CGAAGATTTCCAAGCCAGCG	ATTGGCCCAAGTCCTCCTTG
AMCRX3	AATCCCTGCAGTGGGTCCAA	TTCTTTTGCCTGGCGTTGTG
SLC25A45	CCGAGGAAGGCTGTGTTTCT	ACCACAGCTATGCTGGCAAT
GAPDH	AATGGGCAGCCGTTAGGAAA	GCGCCCAATACGACCAAATC
Prdx4	GATCTCCAAGCCAGCACCTTATT	CCAAGTGGGTAAACTGAGAGTCA
Armxc3	AGGCAAGAGAAGAGGAAGGAAATT	AGTCACTTCAAGGCCACAGTAAT
Slc25a45	GCACCCATTCGACACTGTAAAG	GAAGAAACCCAGGACTGACTCAT
β -actin	GCTGTCCCTGTATGCCTCTG	TTGATGTCACGCACGATTTCCC

analyses were conducted using the Kaplan–Meier method with between-group differences assessed by the Log rank test. A p-value <0.05 was considered statistically significant.

Data Source

Data were collected and consolidated from three Gene Expression Omnibus (GEO) datasets (GSE16134 and GSE23586), comprising 316 samples (72 healthy controls and 244 periodontitis patients). All datasets were generated using the GPL570 platform, facilitating seamless data integration. To address potential heterogeneity arising from integrating multiple patient cohorts, including variations in patient demographics and study protocols, we implemented a comprehensive bioinformatic correction approach. First, non-biological technical variations (batch effects) were adjusted using the ComBat function from the *sva* R package. Furthermore, for differential expression analysis, we incorporated available clinical covariates (such as age and sex where applicable) into the linear models using the *limma* R package to account for potential confounding factors. Raw expression data were processed in R, including probe-to-gene mapping, log₂ transformation, and quantile normalization.

Results

Correlation Analysis Between Periodontitis and Mitochondria, Immunity and Metabolism

We performed a comprehensive transcriptomic analysis of gingival tissue samples from healthy controls (CTL) and periodontitis patients (PD) using the data from the GEO datasets (GSE16134 and GSE23586). After correcting for batch effects with ComBat, PCA revealed clear separation between healthy and periodontitis samples (Figure 1A), indicating distinct gene expression profiles associated with the disease state. Enrichment analysis reveals significant enrichment of multiple mitochondria-related pathways in periodontitis samples than that of controls, highlighting differential expression patterns between the two groups, which underscore the critical role of mitochondrial dysfunction in periodontitis pathogenesis (Figures 1B and S1A, B). Differential expression analysis identified numerous genes with altered expression in PD compared to the CTL group (Figure 1C). Functional enrichment analysis of these differentially expressed genes further illustrates key pathway alterations between CTL and PD samples (Figure 1D). The primary enrichment is related to immune cell and metabolic pathways, indicating that periodontitis is closely linked to immune regulation and metabolic processes. To characterize the immune landscape in periodontitis, we used multiple computational approaches to estimate immune cell composition and activity from the bulk RNA-seq data. CIBERSORT analysis reveals significant differences in immune cell proportions between healthy and periodontitis samples (Figures 1E, F, and S1C–S1E). Notably, plasma cells, naive B cells, and neutrophils are increased in periodontitis, whereas resting dendritic cells, resting mast cells, and macrophages are decreased. Further characterization of the metabolic profiles of periodontitis and control groups via GSVA and ssGSEA reveals significant differences in metabolic pathways (Figures 1G and H). Specifically, the synthesis pathways of glycosaminoglycans such as keratin sulfate are markedly suppressed in the PD group, while pathways related to amino acid and lipid metabolism are significantly upregulated in the PD group. Correlation analysis between mitochondrial and immune-related genes reveals strong associations (Figures 1I, S1F and S1G).

Identification of Periodontitis Molecular Subtypes

To explore potential heterogeneity among periodontitis patients, we performed NMF clustering analysis. Based on the NMF consensus map and other quality metrics, we identified two distinct molecular subtypes of periodontitis, designated as Class 1 (C1) and Class 2 (C2) (Figure S2A–S2C). The glycosaminoglycan pathway is significantly inhibited in GSVA and ssGSEA scores, suggesting that C2 exhibits stromal metabolic defects potentially linked to tissue repair disorders (Figure 2A–D). To investigate differences in mitochondrial function between C1 and C2 groups, we performed the CIBERSORT algorithm (Figure 2E). Interestingly, significant mitochondrial function differences between C1 and C2 (Figure 2F) were observed. In the C2 group, mitochondrial fission, autophagy, and fusion are upregulated, whereas mitochondrial immune responses and mitochondrial organelle contact sites are downregulated. The CIBERSORT

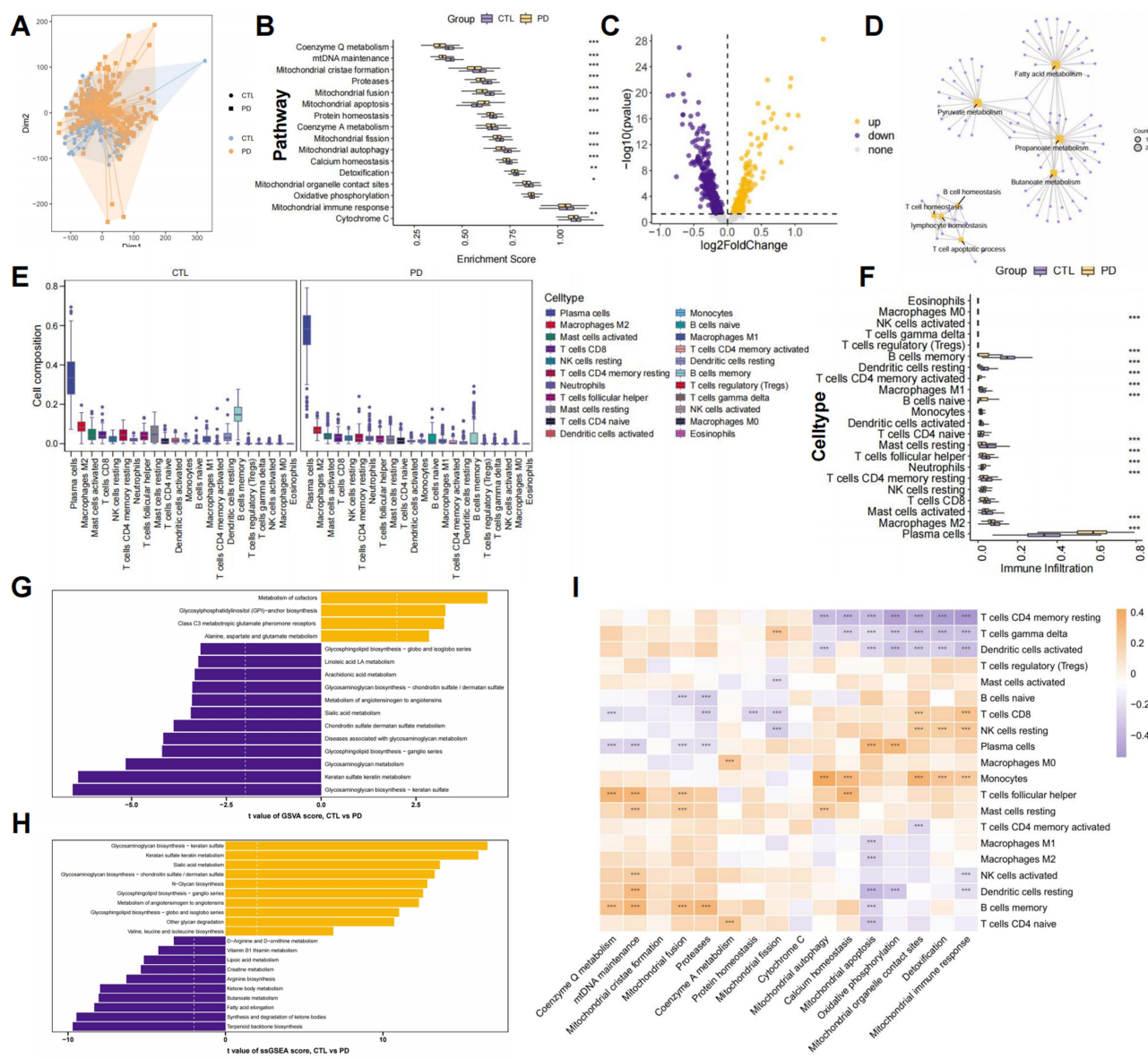


Figure 1 Correlation analysis between periodontitis, mitochondrial dysfunction, and immune cells. **(A)** PCA plot of batch-corrected data distinguishing healthy control (CTL, blue) and periodontitis (PD, Orange) samples, revealing clear separation between groups. **(B)** Enrichment analysis results of the mitochondria-related pathway. **(C)** Volcano plot of differentially expressed genes (DEGs) between healthy and periodontitis samples. Significantly upregulated (orange) and downregulated (purple) genes in periodontitis are highlighted (adjusted p -value < 0.05). **(D)** Function analysis of differential genes between healthy and periodontitis samples. **(E and F)** Boxplots showing immune cell composition in healthy and periodontitis samples as estimated by xCell **(E)** and CIBERSORT **(F)** algorithms. **(G and H)** Bar plots showing \log_2 fold change of immune cell types between healthy and periodontitis samples for GSEA **(G)** and ssGSEA **(H)** results. **(I)** Correlation analysis between mitochondrial function scoring and immune cell based on the CIBERSORT algorithm. * $p < 0.05$, ** $p < 0.01$, *** $p < 0.001$.

analysis results reveal significant differences in immune cell proportions between C1 and C2 groups (Figure 2G and H). Notably, memory B cells, resting mast cells, follicular helper T cells, and naive T cells increase in C2, while naive B cells, resting natural killer (NK) cells, and CD8+ T cells are decreased. Further characterization of the immune features of these subtypes using xCell and ssGSEA reveals significant differences in immune-related gene set activities (Figure 2I–L). Class 2 exhibits higher expression of genes associated with NK and regulatory T cells, whereas Class 1 exhibits elevated expression of genes related to macrophages, Th1 cells, and human leukocyte antigen (HLA) molecules. These distinct immune profiles might have important implications for disease progression and therapeutic responses across patient subgroups.

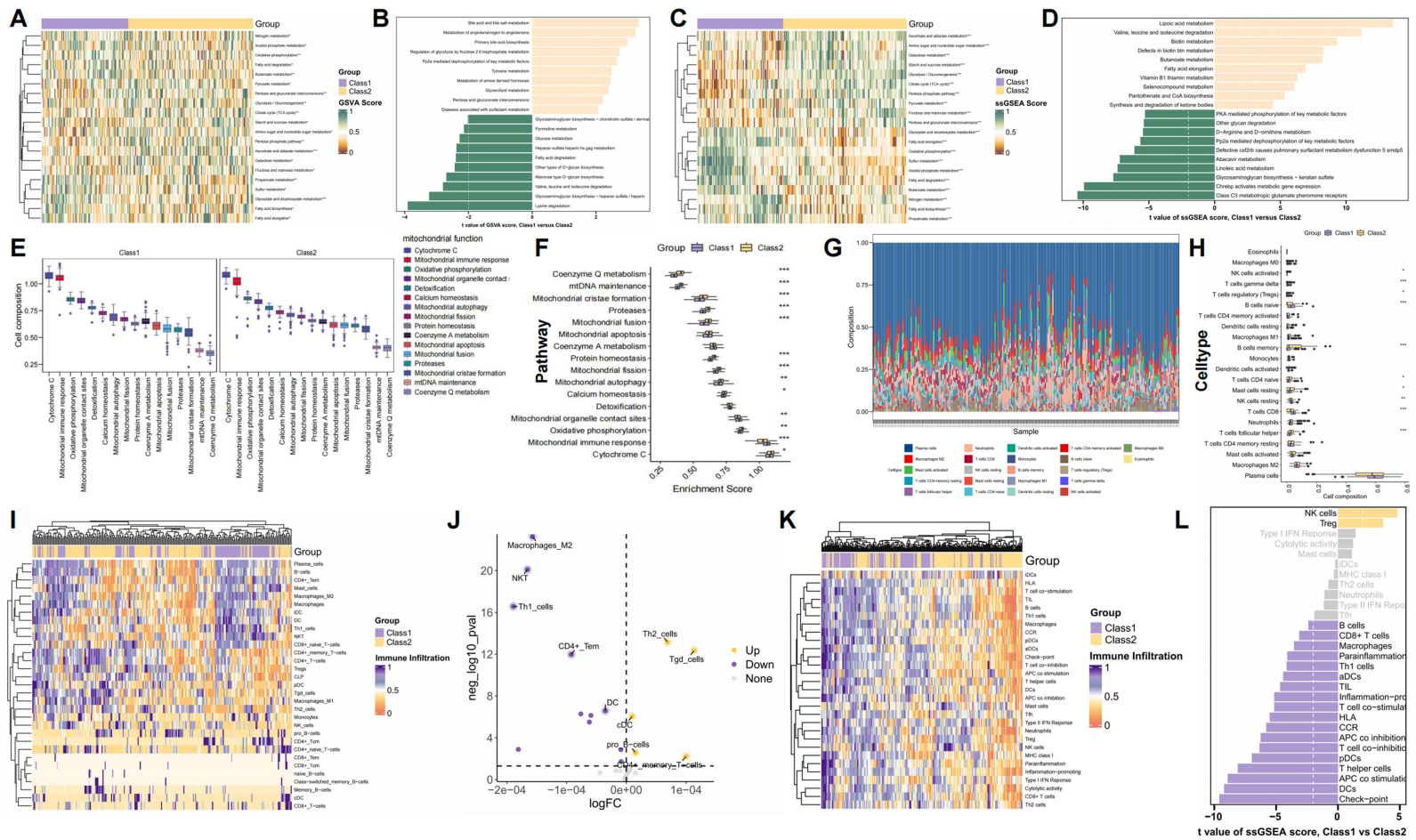


Figure 2 Identification of periodontitis molecular subtypes. **(A–C)** Heatmap of GSEA and ssGSEA scores for MitoDEGs across all samples, clustered by NMF subtypes. **(B–D)** Bar plot showing the mean difference in GSEA and ssGSEA scores between C1 and C2 subtypes for MitoDEGs. **(E and F)** Box plots showing mitochondrial function with significant differences ($p < 0.05$) between C1 and C2 groups as determined by CIBERSORT. **(G)** Stacked bar plot depicting relative proportions of immune cell types across samples based on CIBERSORT analysis. Each bar represents a sample, with colors indicating different cell types. **(H)** Boxplots showing immune cell composition in C1 and C2 as estimated by CIBERSORT algorithms. **(I)** Heatmap of xCell scores for immune-related gene sets across all samples, clustered by NMF subtypes. **(J)** Volcano plot illustrating the differential analysis results of immune-related gene sets between C1 and C2 subtypes. **(K)** Heatmap of ssGSEA scores for immune-related gene sets across all samples, clustered by NMF subtypes. **(L)** Bar plot showing the mean difference in ssGSEA scores between C1 and C2 subtypes for each immune-related gene set. * $p < 0.05$, ** $p < 0.01$, *** $p < 0.001$.

Identification of PRDX4 Based on Multiple Machine Learning Algorithms

To further elucidate the gene expression patterns associated with periodontitis, we performed WGCNA on the differentially expressed genes between healthy and periodontitis samples (Figures 3A and S3A–D). This analysis identified several gene modules with significant correlations to the disease state. The brown module shows a strong positive correlation with periodontitis, likely representing coregulated gene networks that play key roles in disease pathogenesis. By intersecting these genes with NMF-derived genes, we identified seven candidates (Figure 3B). To further prioritize the most critical gene, we systematically evaluated these candidates using 10 machine learning algorithms. Notably, PRDX4 emerged as the top consensus gene, ranking as the most important feature in seven out of ten models (Figure 3C and 3G–M). All ten models demonstrated robust predictive performance on the training set (Figures 3D–F and S4A–S4C). Although ARM CX3 and SLC25A45 were identified as relatively important by the three models, RT-qPCR validation revealed that PRDX4 exhibited the most significant upregulation in periodontitis than the controls (Figures 3N and S4D–S4F). This finding was further corroborated by immunofluorescence, which demonstrated pronounced PRDX4 protein upregulation in periodontitis tissues (Figure 3O). Collectively, these results establish PRDX4 as the most relevant mitochondrial dysfunction–associated gene in the progression of periodontitis.

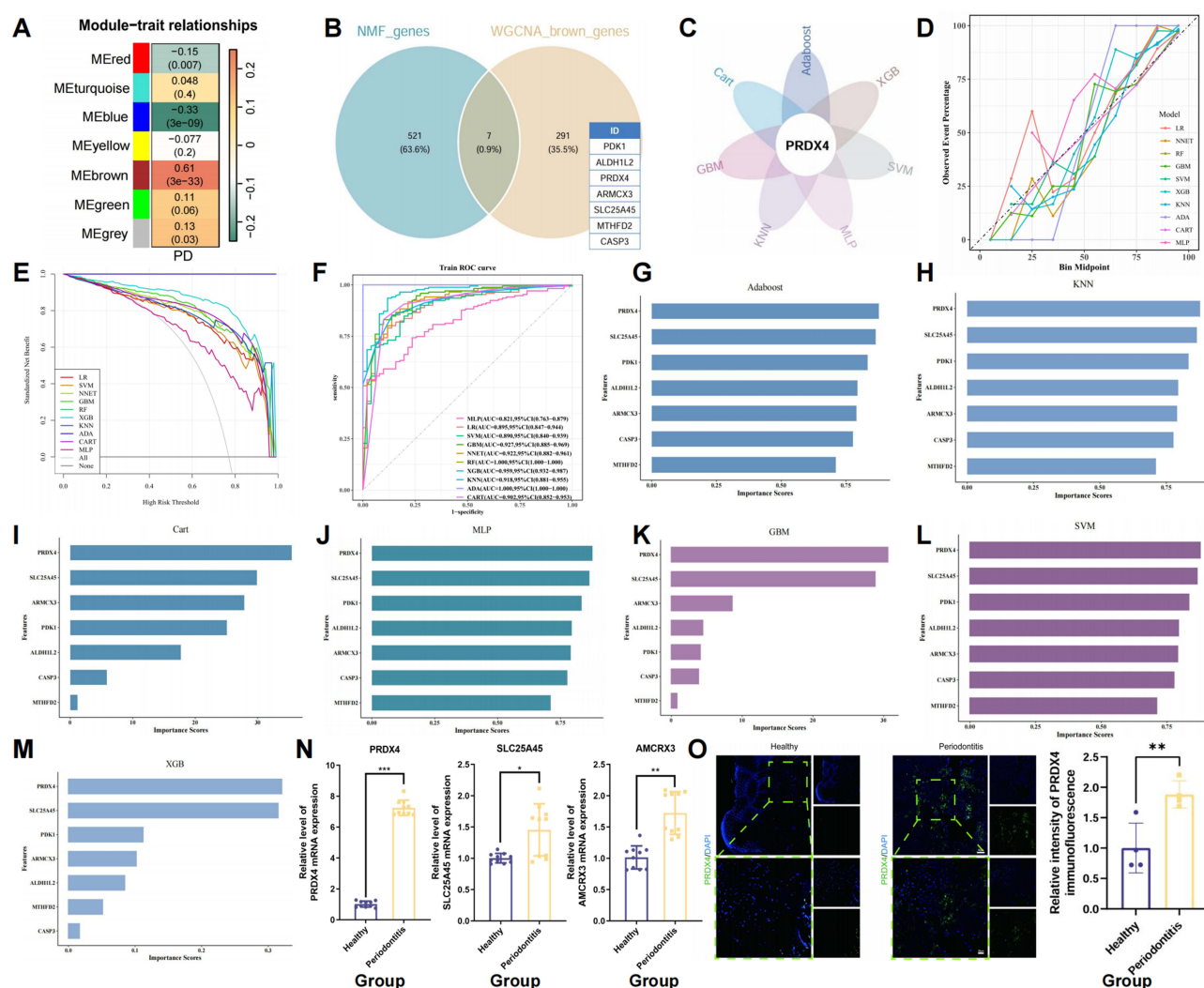


Figure 3 Machine learning model performance and feature importance analysis for PD prediction. (A) Heatmap of module-trait relationships. Each row corresponds to a module eigengene, and the column represents the disease trait (periodontitis). (B) Venn diagram showing overlap of significantly differentially gene identified by NMF and WGCNA brown module. (C) Flower plot showing overlapping gene (PRDX4) based on seven machine learning algorithms. (D) Observed versus predicted probability plots for ten machine learning models on the training set. (E) Precision-Recall curves for the training set. (F) Receiver Operating Characteristic (ROC) curves for the training set. (G–M) Machine learning algorithms to determine the genes most linked to prognosis. (N) RT-qPCR analysis of gene expression in healthy and periodontitis tissues. (O) Fluorescence localization of PRDX4 in healthy and periodontitis tissues. **p* < 0.05, ***p* < 0.01, ****p* < 0.001.

Pseudotime Analysis Reveals the Coordinated Expression of Mitochondrial and Immune Genes During Periodontitis Progression

To gain insights into the temporal dynamics of gene expression during periodontitis progression, we performed pseudotime analysis using a B-spline curve fitted to all genes (Figure 4A). The results indicate that the C2 subtype corresponds to the late stage of periodontitis. Pseudotime analysis further simulated gene expression trends during periodontitis progression, revealing that metabolic and HLA-related genes display increased expression in the late stage (C2 group) (Figure 4B and C). Temporal expression profiles of a representative mitochondrial gene (PRDX4) and B cell

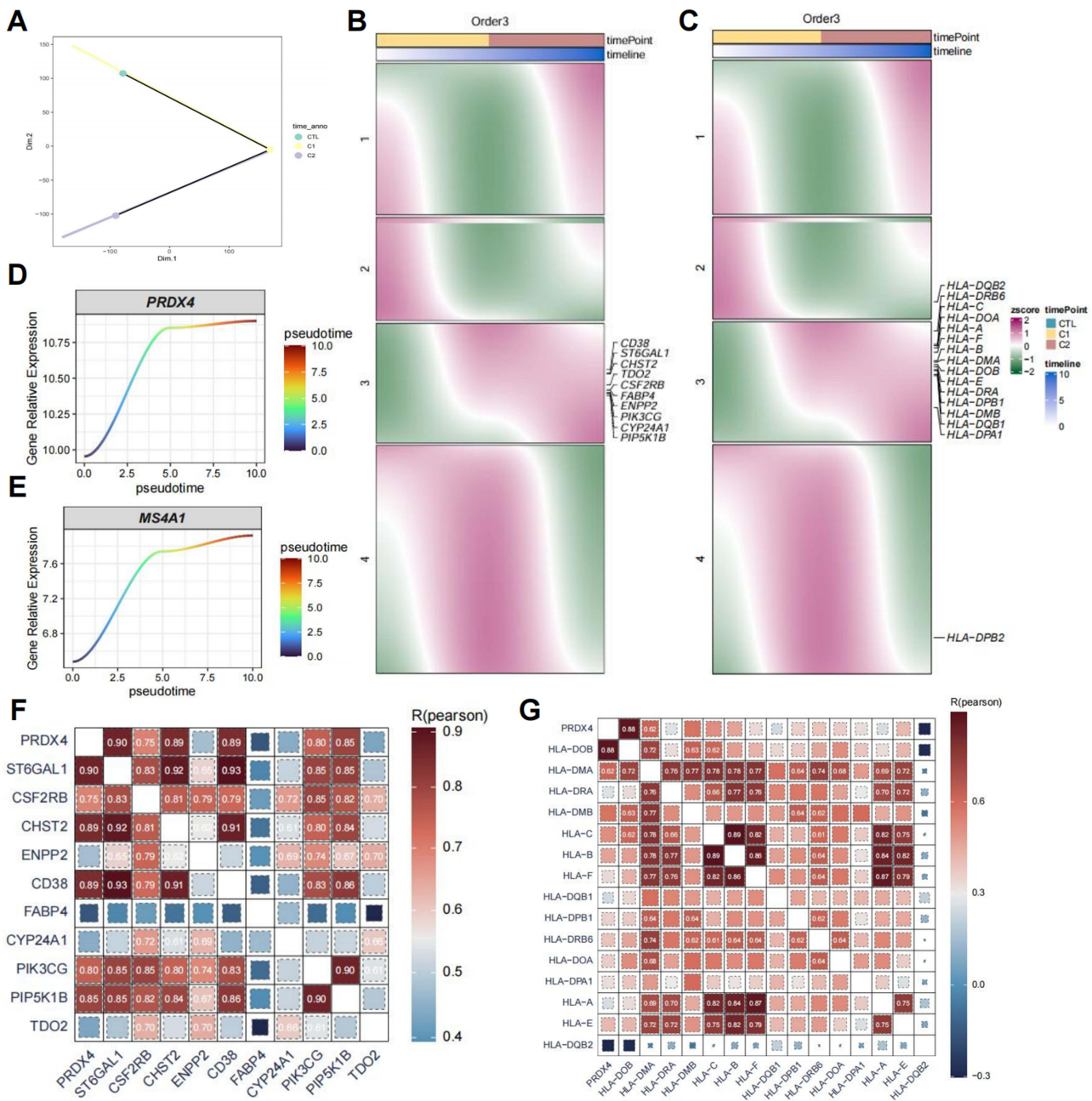


Figure 4 Pseudotime Analysis Reveals Coordinated Expression of Mitochondrial, and Immune Genes During Periodontitis Progression. **(A)** PCA plot of samples fitted with a B-spline curve, illustrating the trajectory of disease progression. Each point represents a sample, with colors indicating different clinical groups (healthy, NMF C1, and NMF C2). **(B and C)** Pseudotime heatmaps of gene expression across three different orderings of samples. **(D and E)** Temporal expression profiles of representative mitochondrial gene (PRDX4) and immune-related genes (MS4A1) across pseudotime. **(F and G)** Correlation heatmap between mitochondrial, metabolic and immune-related genes.

marker (MS4A1) also show elevated expression as the disease advanced (Figure 4D and E). Correlation analysis between mitochondrial and immune-related genes reveals strong associations (Figure 4F and G). Collectively, these findings suggest that PRDX4 might drive periodontitis progression by modulating immune cell responses, particularly B cell-mediated immunity.

Functional Annotation and Immune Microenvironment Correlations of PRDX4 in Periodontitis

Periodontitis patients were grouped according to PRDX4 expression levels, and GO and KEGG enrichment analyses were performed on the resulting differentially expressed genes to elucidate associated biological functions (Figure 5A). Most genes were highly enriched in B cell receptor signaling pathways, as revealed by GSEA results (Figure 5B). To further characterize the immune landscape associated with PRDX4, we performed detailed immune cell infiltration analyses using CIBERSORT and xCell algorithms (Figure 5C–F). The Spearman correlation analysis results show that PRDX4 is positively correlated with mitochondrial apoptosis but negatively correlated with mitochondrial fusion and mtDNA maintenance (Figure 5G). The PRDX4 high-expression panel showed significant upregulation of pathways related to N-glycan biosynthesis, sialic acid metabolism, starch and sucrose metabolism, and folate and pterine metabolism (Figure 5H and I). These metabolic differences might reflect distinct cellular states or energy requirements of the PRDX4 high-expression group, potentially influencing their inflammatory and immune responses.

scRNA-Seq Analysis Unveils Cellular Heterogeneity in Periodontal Tissues

To further characterize the cellular composition and gene expression patterns at single-cell resolution, we analyzed scRNA-seq data from periodontal tissue samples of periodontitis patients and controls (Figure 6A). After quality control and preprocessing, we identified eight distinct cell populations: B, endothelial, epithelial, keratinocytes, mesenchymal stem cells (MSCs), myeloid cells, pericytes, and T/NK cells (Figure 6B). Cell type-specific marker genes were used to annotate these populations (Figure 6C), and their relative proportions were quantified in periodontitis and control samples (Figure 6B). We observed significant differences in cellular composition between periodontitis and control samples, with B cells showing a marked decrease (30.0% vs 70.0%) in periodontitis. scRNA-seq analysis further reveals that PRDX4 is significantly upregulated in periodontitis samples compared to controls and is predominantly enriched in B cell subsets (Figure 6D and E), validating the bulk RNA-seq findings and reinforcing the strong association between PRDX4 expression and B cell involvement in periodontitis pathogenesis.

PRDX4 Expression Dynamics in B Cell Differentiation

Spatial transcriptomic analysis corroborated the scRNA-seq results at the tissue level. PRDX4-high expression regions showed significant overlap with areas enriched for B cell, directly providing in situ evidence for the specific upregulation of PRDX4 in B cell populations identified by single-cell analysis (Figures 7A–7C and S5A–S5D).

Further analysis of B cell subpopulations identified four distinct subsets: plasma, memory B, naive B, and proliferating B cells (Figure 7D–F). The proportions of these subpopulations differed between periodontitis and control samples, with naive B cells showing a significant increase in periodontitis (Figure 7G). Comparison of PRDX4 expression between control and periodontitis conditions in different B cell subtypes showed significant upregulation in plasma cells and memory B cells in the periodontitis group (Figures 7H–I and S6A–S6C), suggesting a potential role for PRDX4 in functional alterations of these subsets during disease progression. Immunofluorescence staining further demonstrated colocalization of PRDX4 with CD20 in periodontitis tissues (Figure 7J). Additionally, we identified a cluster of genes (Cluster 3) with expression patterns similar to PRDX4, characterized by increased expression in late pseudotime (Figure 7K). Functional enrichment analysis of this cluster revealed significant enrichment in pathways related to immune response regulation and activation, including the immune response-regulating cell surface receptor signaling pathway and immune response-activating cell surface receptor signaling pathway, suggesting that PRDX4 might be part of a coordinated gene program involved in B cell activation and immune regulation. To investigate the dynamics of PRDX4 expression during B cell differentiation, we reconstructed the pseudotime trajectory of B cell differentiation (Figures 7L and S6D–S6H). Pseudotime-dependent gene expression analysis demonstrates

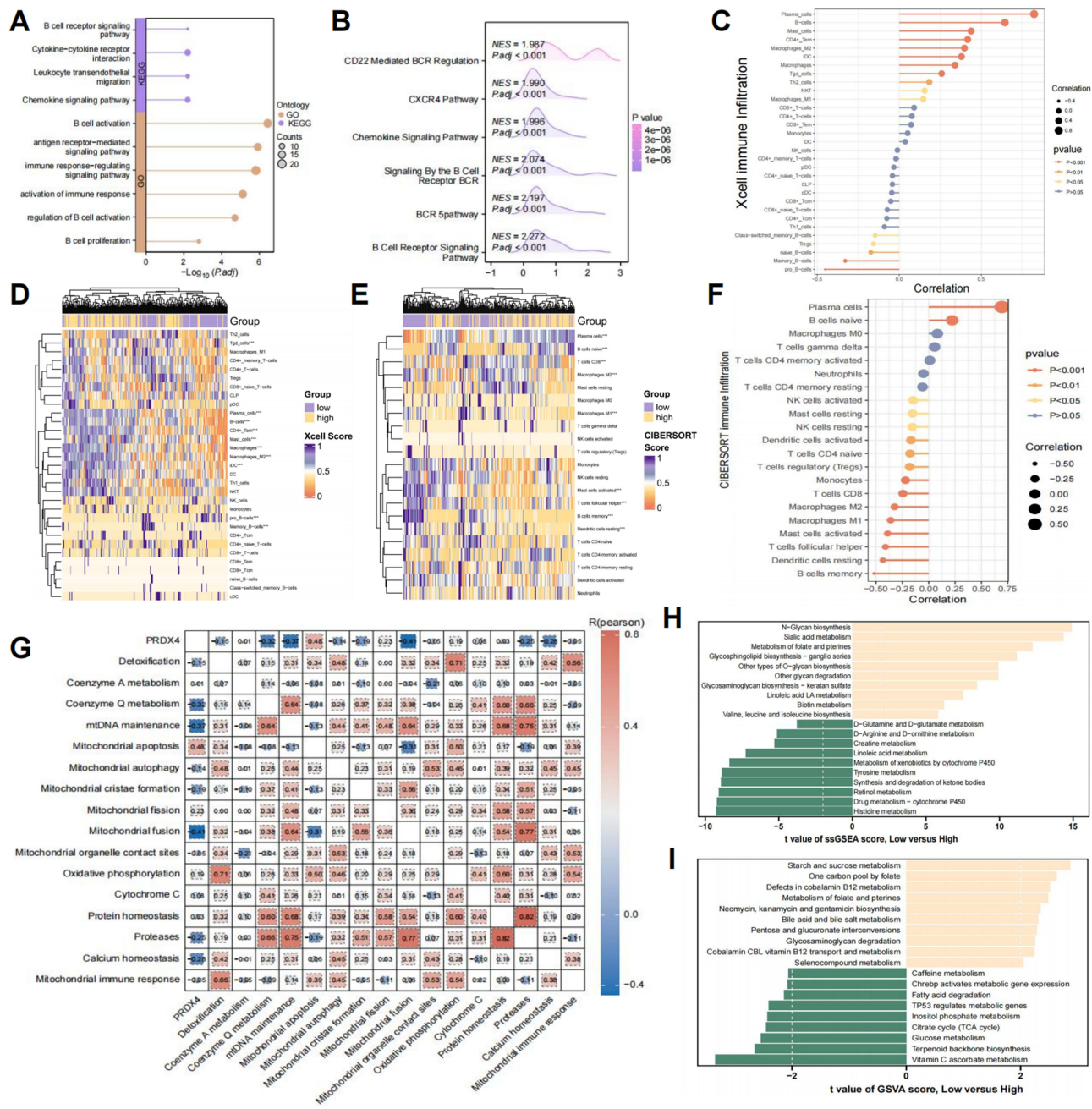


Figure 5 Functional annotation and immune microenvironment correlations of PRDX4 in periodontitis. **(A)** The bubble graph of GO and KEGG functional enrichment analysis in periodontitis. **(B)** GSEA of molecular pathways associated with PRDX4 expression status. **(C)** Correlation between xCell and PRDX4 expression. **(D and E)** Heatmap of CIBERSORT and xCell scores for immune-related gene sets across all samples. **(F)** Correlation between CIBERSORT and PRDX4 expression. **(G)** Correlation heatmap between mitochondrial function and PRDX4. **(H and I)** Bar plots displaying top differentially regulated metabolic pathways with PRDX4 expression status, determined by ssGSEA **(H)** and GSVA **(I)** algorithms.

that PRDX4 expression increases as B cells progress through their differentiation trajectory, with higher expression in more differentiated states compared with other genes (Figure 7M). This pattern suggests a potential role for PRDX4 in B cell maturation and function.

Verification of PRDX4 in the Periodontal animal Model and Drug Sensitivity

We validated PRDX4 expression in a periodontal animal model. Compared with the control group, mice with periodontitis presented significantly aggravated alveolar bone loss, as reflected by a large bone loss area and reduced bone

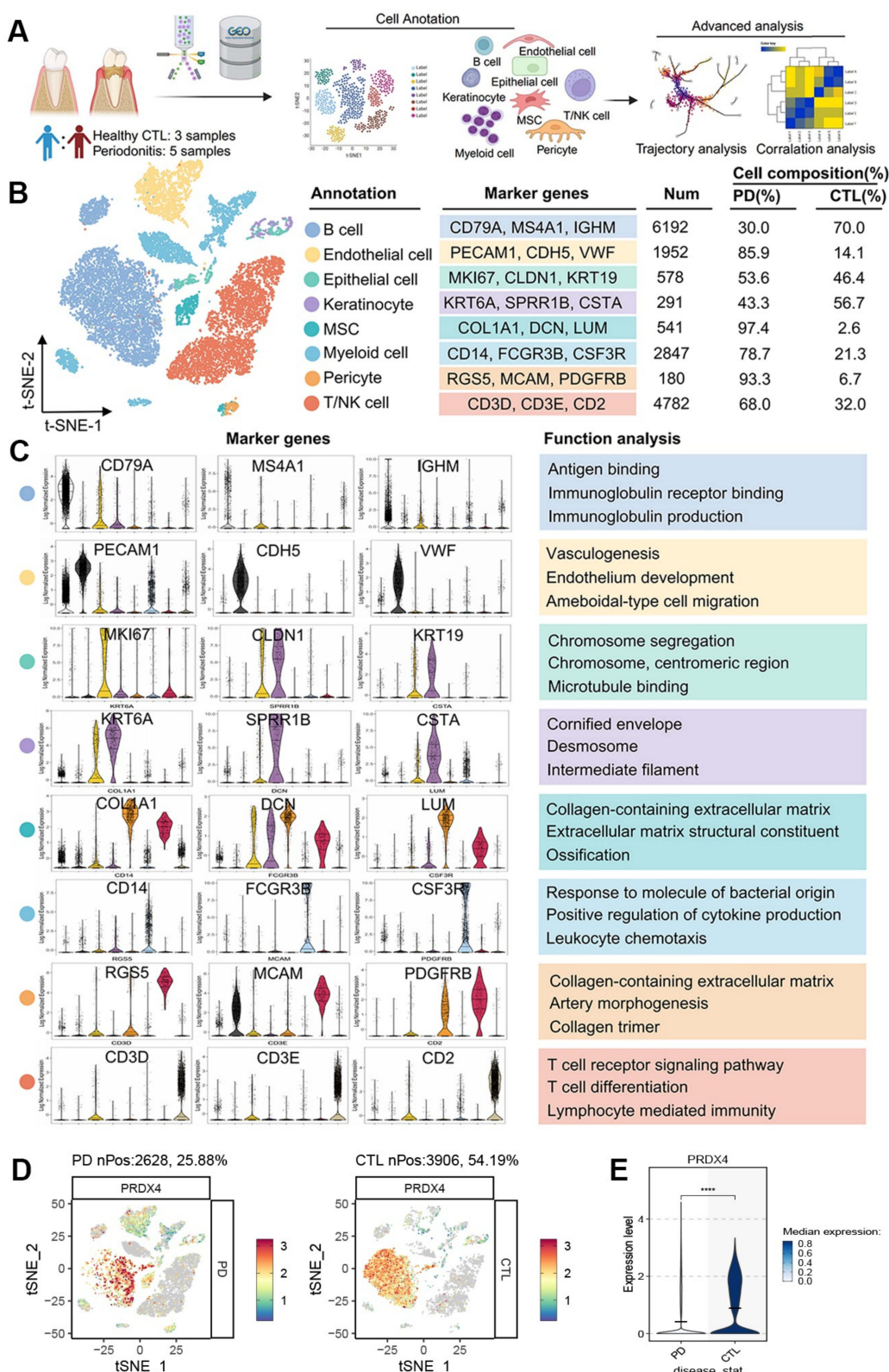


Figure 6 scRNA-seq Analysis Unveils Cellular Heterogeneity in Periodontal Tissues. **(A)** Schematic representation of the single-cell RNA sequencing workflow. **(B)** t-SNE visualization of 17,363 high-quality single cells from periodontal tissues, colored by cell type annotations. **(C)** Violin plots depicting the expression patterns of key marker genes across different cell types and functional analysis of major cell types based on GO enrichment. **(D)** t-SNE plots illustrating the expression distribution of PRDX4 across all cells. **(E)** Violin plots comparing the expression levels of PRDX4 between healthy and periodontitis samples.

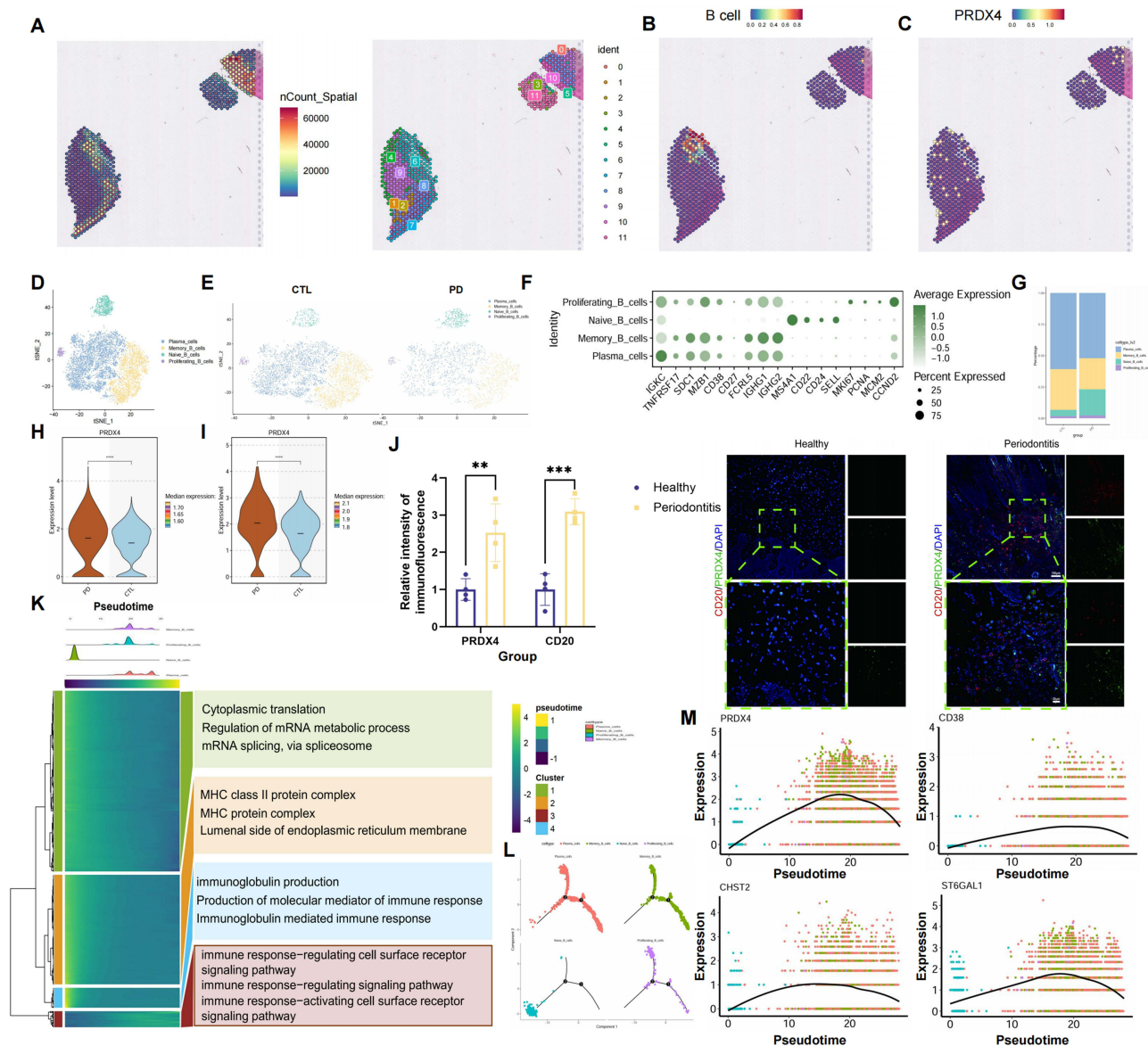


Figure 7 Comprehensive analysis of PRDX4 expression and its role in B cell differentiation. (A) Left: Spatial distribution of total UMI counts (nCount_Spatial) across the tissue section. Right: Unsupervised clustering of spots based on transcriptome profiles. (B) Spatial distribution of B-cell abundance. (C) Projection of PRDX4 expression levels onto the spatial map. (D–E) t-SNE plot and celltype summarizing B cell subpopulations. (F) Heatmap displaying the average expression of marker genes across B cell subpopulations. Color intensity represents expression levels, while dot size indicates the percentage of cells expressing each gene. (G) The proportion of different cell clusters in healthy and periodontitis patients. (H and I) Differential expression analysis of PRDX4 in CTL and PD conditions across B cell subtypes. (J) Fluorescence localization of PRDX4 and CD20 in healthy and periodontitis tissues. (K) Heatmap of pseudotime-dependent gene expression clusters with associated functional enrichment analysis. (L) Pseudotime-dependent gene expression analysis using Monocle2. (M) Different gene expression pattern across pseudotime. *p < 0.05, **p < 0.01, ***p < 0.001.

mineral density (BMD) and bone value/total value (BV/TV) around the ligated tooth (Figure 8A and B). RT-qPCR analysis of mouse periodontal tissues showed expressions of Prdx4, Amcrx3, and Slc25a45 with results indicating a significant upregulation of Prdx4, consistent with our earlier findings (Figure 8C). Immunofluorescence staining further confirmed the colocalization of PRDX4 with B cells in periodontal tissues, suggesting a potential regulatory role of PRDX4 in B cell activity (Figure 8D). Additionally, targeted prediction of traditional Chinese medicines for PRDX4 was performed to explore interactions between relevant herbal medicines and PRDX4 (Figure 8E and F). Drug sensitivity analysis identified aloe as a potential sensitive inhibitor of PRDX4, indicating possible therapeutic effects on mitochondrial dysfunction through PRDX4 targeting.

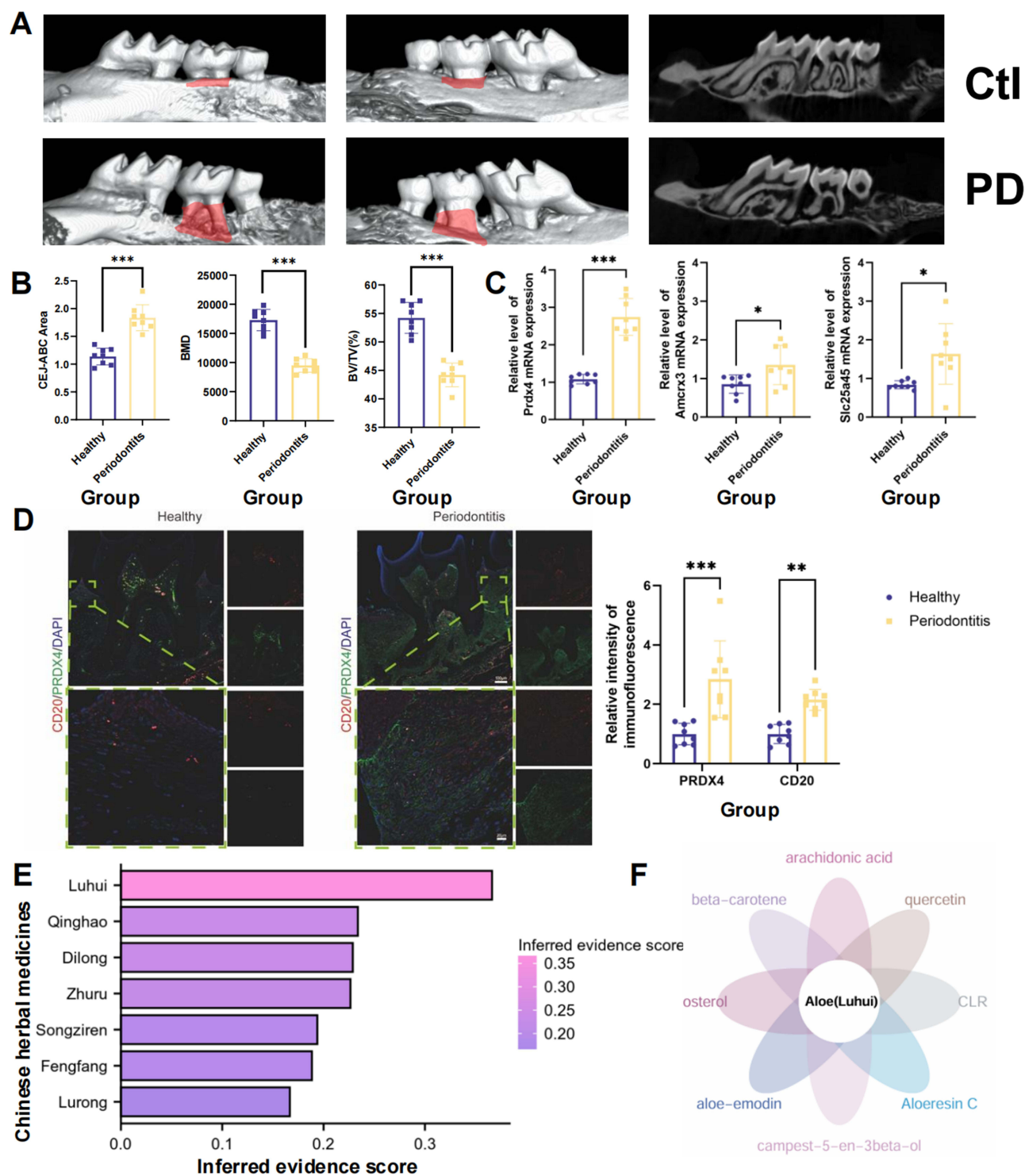


Figure 8 Verification of PRDX4 in periodontal animal model and drug sensitivity. **(A)** Volume microscope and micro-computed tomography (μ CT) images of mesial-distal bone of maxillary alveolar bone in control and periodontitis groups. Periodontitis-induced alveolar bone loss was quantified by measuring the area from the cemental-enamel junction (CEJ) to the alveolar bone crest (ABC) on the buccal and interdental root surfaces around the second molar (the red linear area). **(B)** Bone-related parameters, including CEJ-ABC area, bone mineral density (BMD), and bone value/total value (BV/TV), were quantified. **(C)** The expression levels of different genes between the control and periodontitis groups. **(D)** Fluorescence localization of PRDX4 and CD20 in healthy and periodontitis tissues. **(E)** Evidence scores for the docking of Chinese herbal medicines with PRDX4. **(F)** Flower plot showing overlapping medicinal herb (Aloe) based on database. * $p < 0.05$, ** $p < 0.01$, *** $p < 0.001$.

Discussion

Periodontitis represents a major global health challenge with significant impacts on the quality of life and placing substantial burdens on healthcare systems.³⁷ Current therapeutic approaches, primarily mechanical debridement (scaling and root planning) and adjunctive antimicrobials, face notable limitations.^{9,38,39} While these strategies primarily focus on controlling bacterial infection and inflammation, the underlying molecular mechanisms driving disease progression remain incompletely understood. Within this context, mitochondria have emerged as pivotal players.⁴⁰ Targeting mitochondrial health through strategies such as enhancing biogenesis, reducing oxidative damage, or modulating mitochondrial quality control^{41–44} represent a promising frontier for developing therapies that fundamentally modulate the host response and promote true tissue homeostasis. We aimed to elucidate the role of mitochondria in regulating immune responses and metabolism, providing new mechanistic insights and potential therapeutic targets for the treatment of periodontitis. Through comprehensive transcriptomic analyses integrating bulk and single-cell RNA sequencing data, combined with multiple machine learning algorithms,⁴⁵ we investigated the role of mitochondrial dysfunction in periodontitis progression and uncovered earlier unrecognized links between metabolic reprogramming and alterations in the immune microenvironment.

PRDX4, a typical endoplasmic reticulum–resident 2-Cys antioxidant of peroxiredoxins, can fine-tune hydrogen peroxide catabolism, thereby influencing cell survival through its roles in maintaining redox balance, facilitating oxidative protein folding, and regulating hydrogen peroxide signaling.⁴⁶ Extensive studies have suggested the potential of PRDX4 as a biomarker for various diseases,⁴⁷ including type 2 diabetes, sepsis, atherosclerosis, microalbuminemia, and stroke.^{48–50} However, the role of PRDX4 in periodontitis is not clear. Beyond its canonical function in scavenging hydrogen peroxide and regulating cellular redox balance, PRDX4 also exhibits potent anti-inflammatory properties.⁵¹ It negatively regulates key proinflammatory signaling pathways, notably NF- κ B and inflammasome activation, which are crucial drivers of periodontal tissue destruction.⁴⁸ Importantly, clinical parameters of disease severity such as probing depth, clinical attachment loss, and bleeding on probing positively correlate with established inflammatory markers such as IL-1 β and IL-6.^{52,53} Thus, PRDX4 is a key endogenous protective factor against oxidative and inflammatory damage in the periodontium and a promising therapeutic target and biomarker.

PRDX4 has been reported to modulate mitochondrial events and immune responses in various diseases, highlighting its considerable potential clinical relevance.^{54–56} To validate and expand these findings, our initial bulk transcriptomic analysis of gingival tissues revealed distinct molecular signatures associated with disease progression. Differential expression analysis identified significant dysregulation of genes involved in immune responses and metabolic processes. The GO analysis results of these differentially expressed genes highlighted enrichment in multiple immune-related BPs, particularly B cell receptor signaling and adaptive immune response pathways, suggesting an underappreciated role of adaptive immunity in the pathogenesis of periodontitis.⁴⁸

We next leveraged single-cell RNA sequencing data from periodontal tissues to examine the cellular specificity of these regulatory genes. Through comprehensive transcriptomic analyses integrating bulk and single-cell RNA sequencing data, combined with multiple machine learning algorithms,^{57–59} we investigated the role of mitochondrial dysfunction in periodontitis progression and uncovered previously unrecognized connections between metabolic reprogramming and alterations in the immune microenvironment. Among the subtypes with large differences in mitochondrial function, we also observed considerable differences in immune cell composition and metabolic activity, consistent with reported studies.^{60,61} Our analysis revealed that memory B cells expressed considerably higher levels of PRDX4 compared to naive B cells, while plasma cells exhibited dynamic PRDX4 expression patterns correlated with their differentiation states. Earlier studies demonstrated that PRDX4 plays a crucial role in maintaining cellular redox homeostasis and preventing oxidative stress–induced apoptosis across various cell types. They could regulate NF- κ B signaling and inflammatory cytokine production in immune cells.^{48,51} However, its specific role in B cell differentiation and function remains largely unexplored. Recent evidence indicates that peroxiredoxins, which affect cellular redox homeostasis, can modulate immune responses through redox-dependent and independent mechanisms, underscoring the importance of the relationship between PRDX4 expression and B cell function.^{62,63} Our pseudotime analysis of B cell populations revealed that PRDX4 expression increases during B cell maturation, coinciding with enhanced expression of genes involved in

antibody production and plasma cell differentiation. These findings indicate that PRDX4 might serve as a molecular switch, coordinating metabolic adaptation with B cell differentiation during disease progression.

Compared with Class 1 patients, Class 2 patients characterized by enhanced B cell activation and inflammatory signatures exhibited distinct PRDX4 expression patterns, suggesting that this gene might act as a molecular switch controlling the balance between different disease states. This observation is particularly significant given recent studies showing that redox regulation can influence immune cell fate decisions and inflammatory responses across various disease contexts.^{23,64} Furthermore, our analysis revealed considerable correlations between PRDX4 and metabolic pathways involved in energy metabolism and lipid biosynthesis. While earlier studies have demonstrated that B cell activation and differentiation rely on specific metabolic programs,^{65,66} our results suggest that PRDX4 might serve as a key coordinator of these metabolic adaptations during disease progression. The strong correlation observed between PRDX4 expression and CD20 (a critical regulator of B cell development) further supports this hypothesis and highlights a potential mechanism. Metabolic regulation might influence immune cell function in periodontitis. Additionally, results from the traditional Chinese medicine predictive database identified aloe vera as a potential sensitive inhibitor of PRDX4, with potential effects on mitochondrial function therapy targeting PRDX4. Aloe vera extract has been reported to exhibit anticancer effects on human tongue squamous carcinoma cells *in vitro*⁶⁷ and might represent a promising candidate for the future treatment of periodontitis.

Collectively, these findings elucidate a molecular mechanism by which PRDX4 shapes the immune microenvironment in periodontitis through its influence on B cell differentiation, laying the foundation for developing precision therapeutic strategies targeting PRDX4. Collectively, our findings position oxidative stress as a central nexus connecting mitochondrial dysfunction, immune cell alterations, and tissue damage in periodontitis. The identification of PRDX4—a key antioxidant enzyme—as a hub gene underscores the critical importance of redox imbalance in disease pathogenesis. The PRDX4-high expression profile, associated with specific B cell phenotypes and metabolic alterations, delineates a pathogenic axis wherein mitochondrial-derived oxidative stress drives immune dysregulation through redox-sensitive pathways.

Conclusion

In conclusion, our study delineates a critical pathway in periodontitis pathogenesis wherein mitochondrial dysfunction generates oxidative stress, which in turn drives B cell dysregulation through the key antioxidant regulator PRDX4. We demonstrate that PRDX4 serves as a molecular nexus linking mitochondrial homeostasis to B cell differentiation and function, with its expression dynamically regulated in response to the periodontal oxidative microenvironment. These findings not only elucidate oxidative stress as a central mechanism in periodontitis but also highlight PRDX4 as a promising therapeutic target. Strategies aimed at modulating the PRDX4-mediated antioxidant response may offer a novel approach to mitigating oxidative stress and restoring immune homeostasis in periodontitis.

Data Sharing Statement

Datasets generated and/or analyzed during study are accessed in the GEO database (<https://www.ncbi.nlm.nih.gov/>). The data supporting this study's findings are available from the corresponding author, Mouyuan Sun, upon reasonable request.

Ethics Approval and Consent for Participate

The study methodologies conformed to the standards set by the Declaration of Helsinki. The studies involving human participants were reviewed and approved by the Human Research Ethics Committee in Yongkang First People's Hospital of Wenzhou Medical University (EC2025-LW-016-01(K)). The participants provided their written informed consent to participate in this study. All animal experiments were approved by the Animal Ethics Committee of Zhejiang Center of Laboratory Animals (ZJCLA-IACUC-20011430) and were conducted in accordance with the Guide for the Care and Use of Laboratory Animals (National Research Council, 1996).

Consent for Publication

All patients involved in this study have provided their informed consent for the publication of this manuscript. Additionally, all authors have also given their consent for publication.

Acknowledgments

This work was financially supported by the following programs: National Natural Science Foundation of China (82501180), Zhejiang Provincial Natural Science Foundation of China (LQN25H140004), Zhejiang Province Traditional Chinese Medicine Science and Technology Plan Project (2026ZL0078), China Postdoctoral Science Foundation (2024T170782, 2023M743009), Zhejiang Provincial Medical and Health Science and Technology Plan (2025KY942), Zhejiang University of Stomatology Postdoctoral Scientific Research Foundation (2023PDF013).

Author Contributions

All authors made a significant contribution to the work reported, whether that is in the conception, study design, execution, acquisition of data, analysis and interpretation, or in all these areas; took part in drafting, revising or critically reviewing the article; gave final approval of the version to be published; have agreed on the journal to which the article has been submitted; and agree to be accountable for all aspects of the work.

Disclosure

All authors declare that they have no conflicts of interests.

References

- Genco RJ, Sanz M. Clinical and public health implications of periodontal and systemic diseases: an overview. *Periodontol.* 2020;83(1):7–13. doi:10.1111/prd.12344
- Polizzi A, Nibali L, Tartaglia GM, Isola G. Impact of nonsurgical periodontal treatment on arterial stiffness outcomes related to endothelial dysfunction: a systematic review and meta-analysis. *J Periodontol.* 2025;96:330–345. doi:10.1002/JPER.24-0422
- Hajishengallis G, Chavakis T. Local and systemic mechanisms linking periodontal disease and inflammatory comorbidities. *Nat Rev Immunol.* 2021;21:426–440. doi:10.1038/s41577-020-00488-6
- Eke PI, Thornton-Evans GO, Wei L, Borgnakke WS, Dye BA, Genco RJ. Periodontitis in US adults: national health and nutrition examination survey 2009–2014. *J Am Dent Assoc.* 2018;149:576–588.e6. doi:10.1016/j.adaj.2018.04.023
- Jain N, Dutt U, Radenkov I, Jain S. WHO's global oral health status report 2022: actions, discussion and implementation. *Oral Dis.* 2024;30:73–79. doi:10.1111/odi.14516
- Herrera D, Sanz M, Kerschull M, et al, EFP Workshop Participants and Methodological Consultant. Treatment of stage IV periodontitis: the EFP S3 level clinical practice guideline. *J Clin Periodontol.* 2022;49(24):4–71. doi:10.1111/jcpe.13639
- Kwon T, Lamster IB, Levin L. Current concepts in the management of periodontitis. *Int Dent J.* 2021;71:462–476. doi:10.1111/idj.12630
- Graziani F, Karapetsa D, Alonso B, Herrera D. Nonsurgical and surgical treatment of periodontitis: how many options for one disease? *Periodontol.* 2017;75:152–188. doi:10.1111/prd.12201
- Slots J. Periodontitis: facts, fallacies and the future. *Periodontol.* 2017;75:7–23. doi:10.1111/prd.12221
- Dommisch H, Walter C, Dannewitz B, Eickholz P. Resective surgery for the treatment of furcation involvement: a systematic review. *J Clin Periodontol.* 2020;47(22):375–391. doi:10.1111/jcpe.13241
- Iacobuzio-Donahue CA, Litchfield K, Swanton C. Intratumor heterogeneity reflects clinical disease course. *Nat Cancer.* 2020;1:3–6. doi:10.1038/s43018-019-0002-1
- Govindaraj P, Khan NA, Gopalakrishna P, et al. Mitochondrial dysfunction and genetic heterogeneity in chronic periodontitis. *Mitochondrion.* 2011;11:504–512. doi:10.1016/j.mito.2011.01.009
- Jiang W, Wang Y, Cao Z, et al. The role of mitochondrial dysfunction in periodontitis: from mechanisms to therapeutic strategy. *J Periodontol Res.* 2023;58:853–863. doi:10.1111/jre.13152
- Polizzi A, Alibrandi A, Lo Giudice A, et al. Impact of periodontal microRNAs associated with alveolar bone remodeling during orthodontic tooth movement: a randomized clinical trial. *J Transl Med.* 2024;22:1155. doi:10.1186/s12967-024-05933-x
- Marchi S, Guilbaud E, Tait SWG, Yamazaki T, Galluzzi L. Mitochondrial control of inflammation. *Nat Rev Immunol.* 2023;23:159–173. doi:10.1038/s41577-022-00760-x
- Saunders TL, Windley SP, Gervinkas G, et al. Exposure of the inner mitochondrial membrane triggers apoptotic mitophagy. *Cell Death Differ.* 2024;31:335–347. doi:10.1038/s41418-024-01260-2
- Chen Y, Ji Y, Jin X, et al. Mitochondrial abnormalities are involved in periodontal ligament fibroblast apoptosis induced by oxidative stress. *Biochem Biophys Res Commun.* 2019;509:483–490. doi:10.1016/j.bbrc.2018.12.143
- He P, Liu F, Li M, et al. Mitochondrial calcium ion nanoglutons alleviate periodontitis via controlling mPTPs. *Adv Healthcare Mater.* 2023;12:2203106. doi:10.1002/adhm.202203106
- Sczepanik FSC, Grossi ML, Casati M, et al. Periodontitis is an inflammatory disease of oxidative stress: we should treat it that way. *Periodontol.* 2020;84:45–68. doi:10.1111/prd.12342
- Zaitsev A, Chelushkin M, Dykanov D, et al. Precise reconstruction of the TME using bulk RNA-seq and a machine learning algorithm trained on artificial transcriptomes. *Cancer Cell.* 2022;40:879–894.e16. doi:10.1016/j.ccell.2022.07.006
- Hong Y, Chen Q, Xie H, et al. Multi-omics analysis identifies immune regulatory networks in sepsis-associated liver injury: experimental validation and clinical relevance. *JIR.* 2025;18:10711–10722. doi:10.2147/JIR.S515615
- Lu J, Sheng Y, Qian W, Pan M, Zhao X, Ge Q. scRNA-seq data analysis method to improve analysis performance. *IET Nanobiotechnol.* 2023;17:246–256. doi:10.1049/nbt.12115

23. Sun M, Zhan N, Yang Z, et al. Cuproptosis-related lncRNA JPX regulates malignant cell behavior and epithelial-immune interaction in head and neck squamous cell carcinoma via miR-193b-3p/PLAU axis. *Int J Oral Sci.* 2024;16:63. doi:10.1038/s41368-024-00314-y
24. Hou W, Ji Z, Chen Z, Wherry EJ, Hicks SC, Ji H. A statistical framework for differential pseudotime analysis with multiple single-cell RNA-seq samples. *Nat Commun.* 2023;14:7286. doi:10.1038/s41467-023-42841-y
25. Greener JG, Kandathil SM, Moffat L, Jones DT. A guide to machine learning for biologists. *Nat Rev Mol Cell Biol.* 2022;23:40–55. doi:10.1038/s41580-021-00407-0
26. Francis J, George J, Peng E, Corno AF. The application of artificial intelligence in tissue repair and regenerative medicine related to pediatric and congenital heart surgery: a narrative review. *Regenerative Med Rep.* 2024;1:131. doi:10.4103/REGENMED.REGENMED-D-24-00013
27. Ritchie ME, Phipson B, Wu D, et al. limma powers differential expression analyses for RNA-sequencing and microarray studies. *Nucleic Acids Res.* 2015;43:e47. doi:10.1093/nar/gkv007
28. Wu T, Hu E, Xu S, et al. clusterProfiler 4.0: a universal enrichment tool for interpreting omics data. *Innovation.* 2021;2:100141. doi:10.1016/j.xinn.2021.100141
29. Hänzelmann S, Castelo R, Guinney J. GSEA: gene set variation analysis for microarray and RNA-seq data. *BMC Bioinf.* 2013;14:7. doi:10.1186/1471-2105-14-7
30. Barbie DA, Tamayo P, Boehm JS, et al. Systematic RNA interference reveals that oncogenic KRAS-driven cancers require TBK1. *Nature.* 2009;462:108–112. doi:10.1038/nature08460
31. Pan X, Pan S, Du M, et al. SCMeTA: a pipeline for single-cell metabolic analysis data processing. *Bioinformatics.* 2024;40:btac545. doi:10.1093/bioinformatics/btac545
32. Langfelder P, Horvath S. WGCNA: an R package for weighted correlation network analysis. *BMC Bioinf.* 2008;9:559. doi:10.1186/1471-2105-9-559
33. Gaujoux R, Seoighe C. A flexible R package for nonnegative matrix factorization. *BMC Bioinf.* 2010;11:367. doi:10.1186/1471-2105-11-367
34. Newman AM, Liu CL, Green MR, et al. Robust enumeration of cell subsets from tissue expression profiles. *Nat Methods.* 2015;12:453–457. doi:10.1038/nmeth.3337
35. Zha X. Bioinformatics analysis techniques identify the ferroptosis-related gene MYC as a potential therapeutic target for spinal cord injury: an observational study based on the GEO database. *Advanc Technol Neurosci.* 2025;2:59. doi:10.4103/ATN.ATN-D-24-00026
36. Zhao AR, Yuan R, Kouznetsova VL, Tsigelny IF. Application of machine learning technology and miRNA biomarkers: a novel approach for epilepsy diagnosis. *Advanc Technol Neurosci.* 2025;2:145. doi:10.4103/ATN.ATN-D-25-00017
37. Xu S, Zhang X, Gong R, Huang X, Zhang M. Exploring the correlation between psychological stress, anxiety, and periodontitis among university students: a cross-sectional investigation. *JIR.* 2025;18:8317–8329. doi:10.2147/JIR.S530138
38. Chambrone L, Wang H-L, Romanos GE. Antimicrobial photodynamic therapy for the treatment of periodontitis and peri-implantitis: an American Academy of Periodontology best evidence review. *J Periodontol.* 2018;89:783–803. doi:10.1902/jop.2017.170172
39. Munasur SL, Turawa EB, Chikte UME, Musekiwa A. Mechanical debridement with antibiotics in the treatment of chronic periodontitis: effect on systemic biomarkers—a systematic review. *Int J Environ Res Public Health.* 2020;17:5601. doi:10.3390/ijerph17155601
40. Deng Y, Xiao J, Ma L, et al. Mitochondrial dysfunction in periodontitis and associated systemic diseases: implications for pathomechanisms and therapeutic strategies. *Int J Mol Sci.* 2024;25:1024. doi:10.3390/ijms25021024
41. Bock FJ, Tait SWG. Mitochondria as multifaceted regulators of cell death. *Nat Rev Mol Cell Biol.* 2020;21:85–100. doi:10.1038/s41580-019-0173-8
42. Jang JS, Hong SJ, Mo S, et al. PINK1 restrains periodontitis-induced bone loss by preventing osteoclast mitophagy impairment. *Redox Biol.* 2024;69:103023. doi:10.1016/j.redox.2023.103023
43. He X-T, Li X, Zhang M, et al. Role of molybdenum in material immunomodulation and periodontal wound healing: targeting immunometabolism and mitochondrial function for macrophage modulation. *Biomaterials.* 2022;283:121439. doi:10.1016/j.biomaterials.2022.121439
44. Kummer E, Ban N. Mechanisms and regulation of protein synthesis in mitochondria. *Nat Rev Mol Cell Biol.* 2021;22:307–325. doi:10.1038/s41580-021-00332-2
45. Gao Y, Mu J, Liu K, Wang M. Integrating molecular fingerprints with machine learning for accurate neurotoxicity prediction: an observational study. *Advanc Technol Neurosci.* 2025;2:109. doi:10.4103/ATN.ATN-D-24-00034
46. Jia W, Chen P, Cheng Y. PRDX4 and its roles in various cancers. *Technol Cancer Res Treat.* 2019;18:1533033819864313. doi:10.1177/1533033819864313
47. Schulte J. Peroxiredoxin 4: a multifunctional biomarker worthy of further exploration. *BMC Med.* 2011;9:137. doi:10.1186/1741-7015-9-137
48. Lipinski S, Pfeuffer S, Arnold P, et al. Prdx4 limits caspase-1 activation and restricts inflammasome-mediated signaling by extracellular vesicles. *EMBO J.* 2019;38:e101266. doi:10.15252/embj.2018101266
49. Liang X, Yan Z, Ma W, et al. Peroxiredoxin 4 protects against ovarian ageing by ameliorating D-galactose-induced oxidative damage in mice. *Cell Death Dis.* 2020;11:1053. doi:10.1038/s41419-020-03253-8
50. Homma T, Fujiwara H, Osaki T, Fujii S, Fujii J. Consequences of a peroxiredoxin 4 (Prdx4) deficiency on learning and memory in mice. *Biochem Biophys Res Commun.* 2022;621:32–38. doi:10.1016/j.bbrc.2022.06.096
51. Druso JE, MacPherson MB, Chia SB, et al. Endoplasmic reticulum oxidative stress promotes glutathione-dependent oxidation of collagen-1A1 and promotes lung fibroblast activation. *Am J Respir Cell Mol Biol.* 2024;71:589–602. doi:10.1165/rcmb.2023-0379OC
52. Hajishengallis G. Interconnection of periodontal disease and comorbidities: evidence, mechanisms, and implications. *Periodontol.* 2022;89:9–18. doi:10.1111/prd.12430
53. Nikniaz S, Vaziri F, Mansouri R. Impact of resveratrol supplementation on clinical parameters and inflammatory markers in patients with chronic periodontitis: a randomized clinical trial. *BMC Oral Health.* 2023;23:177. doi:10.1186/s12903-023-02877-4
54. Yamada S, Guo X. Peroxiredoxin 4 (PRDX4): its critical in vivo roles in animal models of metabolic syndrome ranging from atherosclerosis to nonalcoholic fatty liver disease. *Pathol Int.* 2018;68:91–101. doi:10.1111/pin.12634
55. Huang Y, Zhang Y, Liu Y, Jin Y, Yang H. PRDX4 mitigates diabetic retinopathy by inhibiting reactive gliosis, apoptosis, ER stress, oxidative stress, and mitochondrial dysfunction in Müller cells. *J Biol Chem.* 2025;301:108111. doi:10.1016/j.jbc.2024.108111
56. Kam MK, Lee DG, Kim B, et al. Peroxiredoxin 4 ameliorates amyloid beta oligomer-mediated apoptosis by inhibiting ER-stress in HT-22 hippocampal neuron cells. *Cell Biol Toxicol.* 2019;35:573–588. doi:10.1007/s10565-019-09477-5
57. Sun M, Yang Z, Luo Y, et al. Using multiomics and machine learning: insights into improving the outcomes of clear cell renal cell carcinoma via the SRD5A3-AS1/hsa-let-7e-5p/RRM2 axis. *ACS Omega.* 2025;10:25633–25647. doi:10.1021/acsomega.5c01337

58. He D, Yang Z, Zhang T, et al. Multi-omics and machine learning-driven CD8+ T cell heterogeneity score for head and neck squamous cell carcinoma. *Mol Ther Nucleic Acids*. 2025;36:102413. doi:10.1016/j.omtn.2024.102413
59. Zha X. Challenges and opportunities for repairing the injured spinal cord: inflammation, regeneration, and functional reconstruction. *Regenerative Med Rep*. 2025;2(36). doi:10.4103/REGENMED.REGENMED-D-24-00027
60. Tiwari-Heckler S, Robson SC, Longhi MS. Mitochondria drive immune responses in critical disease. *Cells*. 2022;11:4113. doi:10.3390/cells11244113
61. Newman LE, Shadel GS. Mitochondrial DNA release in innate immune signaling. *Annu Rev Biochem*. 2023;92:299–332. doi:10.1146/annurev-biochem-032620-104401
62. Lu J, Holmgren A. The thioredoxin antioxidant system. *Free Radic Biol Med*. 2014;66:75–87. doi:10.1016/j.freeradbiomed.2013.07.036
63. Nicolussi A, D’Inzeo S, Capalbo C, Giannini G, Coppa A. The role of peroxiredoxins in cancer. *Mol Clin Oncol*. 2017;6:139–153. doi:10.3892/mco.2017.1129
64. Weisel FJ, Mullett SJ, Elsner RA, et al. Germinal center B cells selectively oxidize fatty acids for energy while conducting minimal glycolysis. *Nat Immunol*. 2020;21:331–342. doi:10.1038/s41590-020-0598-4
65. Ogishi M, Kitaoka K, Good-Jacobson KL, et al. Impaired development of memory B cells and antibody responses in humans and mice deficient in PD-1 signaling. *Immunity*. 2024;57:2790–2807.e15. doi:10.1016/j.immuni.2024.10.014
66. Gamez-Garcia A, Espinosa-Alcantud M, Bueno-Costa A, et al. A SIRT7-dependent acetylation switch regulates early B cell differentiation and lineage commitment through Pax5. *Nat Immunol*. 2024;25:2308–2319. doi:10.1038/s41590-024-01995-7
67. Chiu T-H, Lai -W-W, Hsia T-C, et al. Aloe-emodin induces cell death through S-phase arrest and caspase-dependent pathways in human tongue squamous cancer SCC-4 cells. *Anticancer Res*. 2009;29:4503–4511.

Clinical, Cosmetic and Investigational Dentistry

Publish your work in this journal

Clinical, Cosmetic and Investigational Dentistry is an international, peer-reviewed, open access, online journal focusing on the latest clinical and experimental research in dentistry with specific emphasis on cosmetic interventions. Innovative developments in dental materials, techniques and devices that improve outcomes and patient satisfaction and preference will be highlighted. The manuscript management system is completely online and includes a very quick and fair peer-review system, which is all easy to use. Visit <http://www.dovepress.com/testimonials.php> to read real quotes from published authors.

Submit your manuscript here: <https://www.dovepress.com/clinical-cosmetic-and-investigational-dentistry-journal>

Dovepress

Taylor & Francis Group